Springer

Journal of Mechanical Science and Technology 23 (2009) 1591~1601

Journal of Mechanical Science and Technology

www.springerlink.com/content/1738-494x
DOI 10.1007/s12206-009-0425-1

Experimental investigation of nanoparticle formation characteristics from advanced gasoline and diesel fueled light duty vehicles under different certification driving modes †

Hyungmin Lee, Juwon Kim, Cha-Lee Myung, and Simsoo Park*

School of Mechanical Engineering, Korea University 1, 5-Ga, Anam-dong, Sungbuk-gu, Seoul 136-701, Korea

(Manuscript Received December 9, 2008; Revised April 1, 2009; Accepted April 9, 2009)

Abstract

This paper mainly focused on the comparison of nanoparticle size distribution and number concentration level characteristics with gasoline and diesel fueled light duty vehicles. In the engine research, particle size distribution and number concentrations were analyzed by a DMS500 with engine parameters. Time-resolved particle number concentration levels from test vehicles were measured by a golden particle measurement system (GPMS) as recommended by a Particle Measurement Programme (PMP) on certification modes such as New European Driving Cycle (NEDC), Federal Test Procedure (FTP)-75, and Highway Fuel Economy Test (HWFET). In addition, particle emission characteristics from vehicles were analyzed by DMS500 during transient and high-speed driving conditions. From the results, we found that the formation of particles was highly dependent on vehicle speed and load conditions for each mode. The diesel vehicle equipped with a particulate filter showed substantial reduction of the total particle number whose number concentration was equivalent to that of the gasoline vehicle. The nucleation mode particles from gasoline fuel were mainly emitted; however, the accumulation mode particles from the diesel fuel were generally analyzed.

Keywords: Nanoparticle; GPMS; Particulate matter; Particulate filter; Nucleation mode; Accumulation mode

1. Introduction

Recently, environmental researchers and the general public have increasingly focused their attention to internal combustion engines. Small particles causing fine dust formation in the atmospheric environment are known to reduce visibility. From epidemiological studies carried out by a number of research groups, particles can have a negative effect on human health [1-4]. In addition, many studies have stated that atmospheric particles comprise one important factor where mortality and morbidity are concerned [5].

Particle number and mass concentration levels from state-of-the-art engines tend to exhaust much lower than older engines. This is a result of improvements in engine design, quality of combustion, fuel spray angle, and atomization of fuel by high pressure injection, as well as the development of advanced technologies for fuel and oil formulations [6-8]. In vehicle exhaust emissions, particulate matter (PM) consists of tiny solid particles and liquid droplets ranging from a few nanometers to around one micrometer in diameter [9].

Among others, the advantages of diesel-powered engines include their ability to increase engine power output, fuel economy, and high durability compared to park ignition engines. Diesel engines are widely used in heavy-duty trucks, buses, and light-duty vehicles as they have fewer penalties in terms of performance and emission [10]. Although diesel engines emit considerably higher concentrations of particulate mass than gasoline engines, the total number of vehi-

† This paper was recommended for publication in revised form by Associate Editor Kyoung Doug Min

*Corresponding author. Tel.: +82 2 3290 3368, Fax.: +82 2 926 9290
E-mail address: spark@korea.ac.kr

cle miles traveled by gasoline-fueled vehicles in urban areas greatly exceeds that of diesels, in which case gasoline vehicles may contribute up to 68% of the vehicle engine-generated particulate mass and 90% of the particulate number [11].

Current PM standards regulate particle emissions in terms of the total mass of PM emitted per kilometer traveled. This regulation is an effective way of controlling larger-sized particle emissions because finer particles contribute little to the total mass of PM emissions [12, 13]. Many studies have shown that, for internal combustion engines, the decrease in total particle number concentration does not accompany the reduction of particle mass. Toward solving such problems, over the past 10 years, efforts have been devoted to the development of a particle measurement method and the analysis of particle characterization through the UN-GRPE Particle Measurement Programme (PMP). This is a collaborative program operating under the auspices of the UNECE (United Nations Economic Commission for Europe) / GRPE (Working Party on Pollution and Energy) group, with the strong involvement of the governments of the UK, Germany, Sweden, France, and lately, Japan and Korea. This program aims to focus on the development of a new approach to PM measurement in vehicle exhaust emissions, which may be used to replace or complement the existing mass-based system used for regulatory purposes [14-17].

The work presented here aims to evaluate particle size distribution characteristics and number concentration levels emitted from gasoline and diesel fueled engines with various operation conditions, as well as light duty vehicles on the NEDC, FTP-75, and HWFE driving modes.

2. Experimental apparatus and methods

2.1 Gasoline and diesel engine experimental system

Figs. 1 and 2 show the schematic diagram of the gasoline and diesel engine experimental apparatus used to analyze the particle number concentration and size distribution characteristics for the start phase and steady operation condition.

The gasoline engine is a double overhead camshaft (DOHC), in-line four cylinder, 2.0 liter SI engine equipped with a continuously variable valve timing (CVVT) device. Fuel injection pressure is constantly controlled to 3.5 bar by the pressure regulator installed inside the fuel pump in the fuel tank and maintained

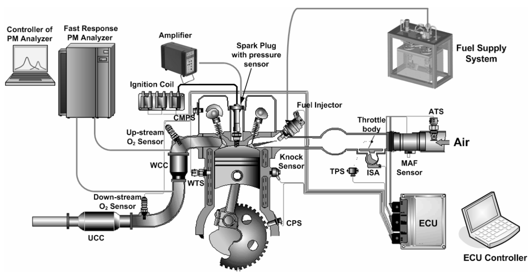

Fig. 1. Schematic diagram of the gasoline engine experimental system.

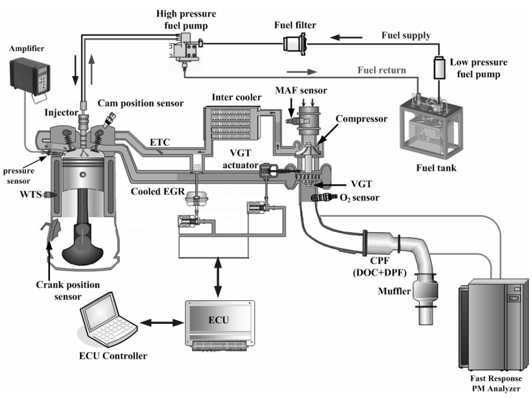

Fig. 2. Schematic diagram of the diesel engine experimental system.

tained through the fuel supply line. The throttle angle is automatically controlled by an electronic servomotor, which can be managed using time steps to eliminate throttle angle variation during fast transient operation. The diesel engine is a single overhead camshaft (SOHC), in-line four cylinder, 2.2 liter variable geometry turbocharged (VGT) common rail direct injection (CRDI) engine with electronic throttle control (ETC) and catalyzed particulate filter (CPF). Fuel is supplied from a fuel tank to a high-pressure pump through a low-pressure pump. The common rail pressure is controlled by a high-pressure pump with engine-operating conditions. Detailed engine specifications are given in Table 1. Particle size distribution and number concentration characteristics are analyzed by a differential mobility spectrometer (DMS500) through an engine test. In the transient test, the engines are decoupled by a dynamometer to simulate a very aggressive transient operation.

2.2 Vehicle experimental system

Two light-duty vehicles meeting which are ULEV

Table 1. Specifications of test engines.

Engine Type	In-line, DOHC 16V (Gasoline)	In-line, SOHC (Diesel)
Displacement	1,998 cc	2,188 cc
Bore x Stroke	86 mm x 86 mm	87 mm x 92 mm
Compression ratio	10.5 : 1	17.3 : 1
Valve timing	IVO: variable, IVC: variable EVO: BBDC 34°CA, EVC: ATDC 10°CA	IVO: BTDC 7°CA, IVC: ABDC 35°CA EVO: BBDC 52°CA, EVC: ATDC 6°CA
Fuel injection	Multi Point Injection	Common Rail Direct Injection
Exhaust system	WCC+UCC	DOC+DPF

Table 2. Specifications of test vehicles.

Vehicles	Gasoline (ULEV)	Diesel (EURO 4)
Engine Type	L4-VVT	L4-VGT
Engine Displacement	1,998cc	1,991cc
Transmission	AT4	AT4
Aftertreatment Equipment	WCC+UCC	DOC+DPF
Injection Type	MPI	CRDI
Max. power (hp/rpm)	144/6,000	151/3,800
Weight empty (kg)	1,460	1,581
Model Year	2007	2008
Odometer (km)	24,586	17,114

and EURO 4 regulations were tested on a chassis dynamometer to evaluate particle number concentration and particle mass emissions under the NEDC, FTP-75, and HWFET modes. The specifications of the test vehicles and the schematic diagrams of the vehicle experimental apparatus are presented in Table 2 and Fig. 3.

The flow rate of the diluted exhaust gas through the constant volume sampler (CVS) tunnel was 20 m^3/min at standard reference conditions (i.e., 20ºC and 1 bar). Relative humidity was constantly maintained around 32% with a thermo-hygrostat. The primary dilution air was allowed to pass through a high efficiency particulate air (HEPA) filter to minimize particle effect in the background level of an emission facility. The number of particles emitted from the test vehicle was counted using the golden particle measurement system (GPMS) upon the recommendation of the PMP. The volatile particle remover (VPR) comprises a first particle number diluter (PND_1), an

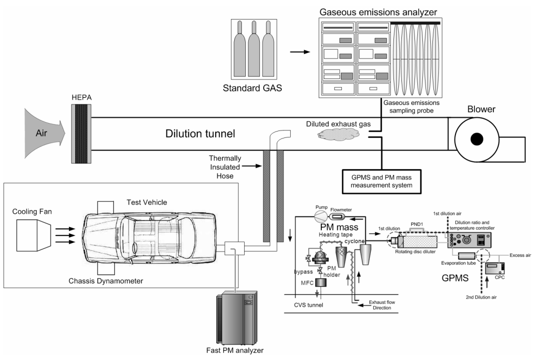

Fig. 3. Schematic diagram of the vehicle experimental system.

evaporation tube (ET), and a PND_2. A sample particle was diluted with the particle-free dilution air at 150°C inside the rotating disc diluter (MD19-2E). After the first dilution, the sample flow was moved to the ET, which was maintained at a temperature of 300°C. A 3010D condensation particle counter (CPC) manufactured by TSI was used to measure the time-resolved particle number concentrations at three different driving modes. In addition, a DMS500 fast particulate spectrometer was installed at the tail pipe location to analyze the particle number characteristics under transient and steady driving tests (from 80 km/h to 120 km/h). To minimize fuel variation during the test periods, gasoline and diesel fuels were supplied from the same filling station with one batch preparation. The octane number and sulphur contents were 93.2 and 18 mg/kg for gasoline fuel, respectively, while the cetane number and sulphur contents were 55.9 and 6 mg/kg for diesel fuel, respectively.

3. Engine experimental results

3.1 In-cylinder pressure characteristics for gasoline and diesel engines

A combustion analyzer with a spark plug-type sensor for gasoline engine and a glow plug-type sensor for diesel engine was used to analyze the in-cylinder pressure of the No. 1 cylinder. In-cylinder pressure was continuously measured throughout 200 cycles, after which the average value was obtained. Spark timings for the gasoline engine varied from BTDC 50°CA to BTDC 20°CA in 10°CA units, while the fuel injection timings of the diesel engine were adjusted between BTDC 6°CA and ATDC 9°CA in 3°CA intervals. In-cylinder pressure traces with various spark timings and fuel injection timings are presented in Figs. 4 and 5. In case of the gasoline engine,

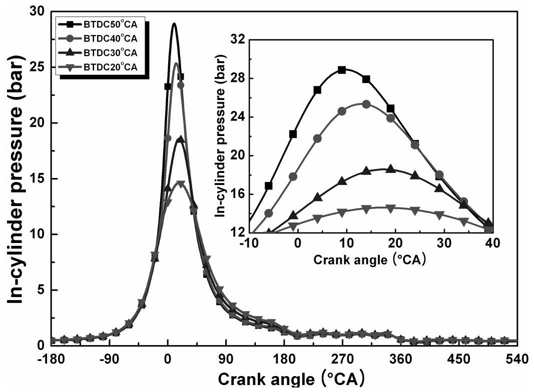

Fig. 4. In-cylinder pressure characteristics with various spark timings of the gasoline engine. Test conditions are λ=1.0, IVO=BTDC 35°CA, 2,400 rpm, BMEP 3.0 bar, and a fully warmed up condition.

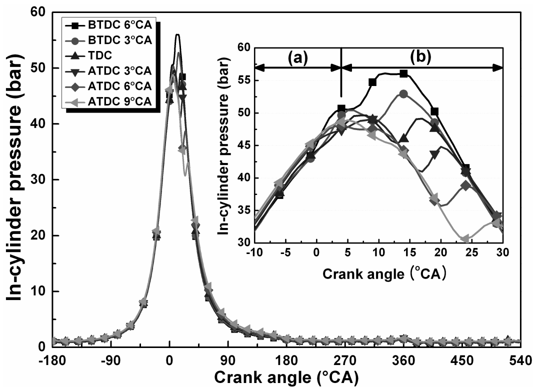

Fig. 5. In-cylinder pressure characteristics with various injection timings of diesel engine. Test conditions are 1,400 rpm, BMEP 4.0 bar, and a fully warmed up condition.

the value and location of the peak cylinder pressure for BTDC 20°CA are about 15 bar and ATDC 20°CA, respectively, while those for BTDC 50°CA are about 29 bar and ATDC 10°CA.

On the other hand, the in-cylinder pressure values of the diesel engine are higher than those of the gasoline engine. The value and location of the peak cylinder pressure for BTDC 6°CA are about 55 bar and ATDC 15°CA, respectively, while those for ATDC 9°CA are about 47 bar and ATDC 5°CA. Curve (a) shows the increasing cylinder pressure by compression stroke, and curve (b) indicates the cylinder pressure profiles by main fuel injection. As the spark timing and fuel injection timing become advanced, in-cylinder pressure is gradually increased because the combustion quality is improved for the gasoline engine and the premixed combustion phase is shortened for the diesel engine [18].

3.2 Particle size distribution and number concentrations with engine parameters at steady condition

Generally, PM size distributions are classified as trimodal, mainly consisting of the nucleation, accumulation, and coarse modes. These modes are distinguished by the particle diameter, with the nucleation mode being less than about 50 nm and the accumulation mode ranging from 50 to 1000 nm. Finally, the coarse mode rarely emitted in an internal combustion engine is composed of particles with diameters greater than 1000 nm [9]. Fig. 6 shows the particle size distribution and number concentration behavior with excess air ratio (λ) and spark timings for the gasoline engine at a steady operating condition. The highest particle emissions were measured at a rich operating condition (λ=0.8). From the test result, it can be seen that the nucleation mode was largely emitted more than the accumulation mode. In the case of lambda of 0.8, the nucleation and accumulation modes are over one order of magnitude higher than that of lambda of 1.2.

As spark timing advanced from BTDC 20°CA to BTDC 50°CA, the particle number concentrations also increased. The PM number concentrations at BTDC 50°CA are over one order of magnitude higher than that of BTDC 20°CA, which is around 10 nm. However, the particle number concentration over the range of spark timing test was not distinctively observed compared to the mixture ratio. The effect of PM number reduction by retarding spark timing can be explained by the exhaust gas temperature. The exhaust gas temperature is highest for late spark timing, so particle number levels as well as THC concentrations decrease because the amount of post-flame oxidation is increased by retarded spark timing [19].

The effect of the aftertreatment for gasoline and diesel engines on the particle size distribution and number concentration characteristics is presented in Fig. 7. The PM size distribution measured in the gasoline engine was bi-modal, consisting of the nucleation and accumulation modes. When compared with the upstream and downstream particle number concentrations, an order of magnitude is similar at various load conditions except at BMEP 4.0 bar. Particle number concentrations with diameters around 10 nm were largely emitted. On the BMEP 4.0bar condition, such particle number concentrations decreased a

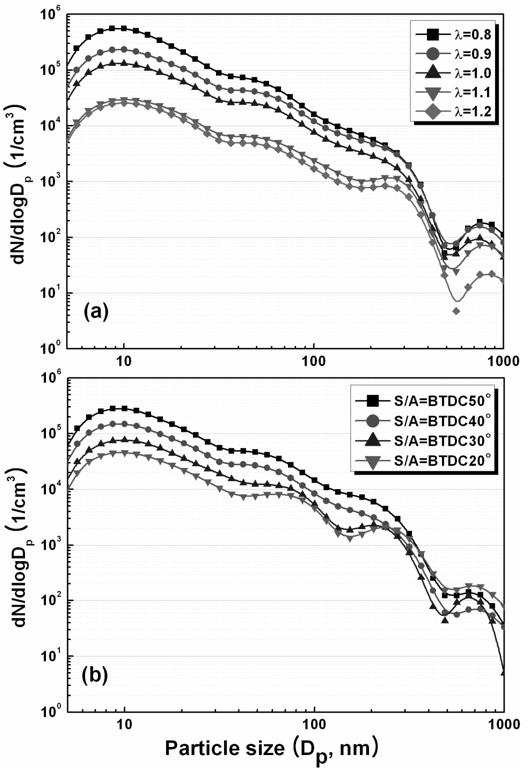

Fig. 6. Particle size distribution and number characteristics for gasoline engine: (a) Air-fuel ratio; (b) spark timings. Test conditions are 2,400 rpm, BMEP 3.0bar, and a fully warmed up condition.

maximum of two times at the downstream of the catalytic converter.

Fuel injection timing for the diesel engine varied by increments of 3°CA units from BTDC 6°CA to ATDC 9°CA, while engine operation conditions (BMEP 4.0bar at 1,400 rpm) remain fixed. As the fuel injection timing was retarded from BTDC 6°CA to ATDC 9°CA, nucleation mode levels decreased along with the increase in accumulation mode concentration levels. Accumulation mode particles mainly consist of carbonaceous agglomerates generated shortly after the start of combustion. Retarded fuel injection timing at a low part load condition results in an incomplete combustion, leading to an increase in unburned hydrocarbons. In addition, injection timing affects the residence time for primary soot particle oxidation. As injection timing is advanced, accumulation mode particles are supposed to be reduced due to an increase of residence time for soot oxidation.

3.3 Particle size distribution and number concentrations during the start phase

Time-resolved particle size spectra characteristics during cold start and fast transient operations using DMS500 for gasoline and diesel engines are illustrated in Fig. 8. From the particle spectra, the nucleation mode was mostly emitted by the gasoline-fueled engine, while the accumulation mode was observed in the upstream of DPF for the diesel engine.

In Fig. 9, nucleation and accumulation modes are widely distributed and largely emitted during cold start and fast acceleration. Particle number concentrations were emitted a maximum of 3.0E+8 particles/cm^3 at the upstream of DPF, and a maximum of 1.0E+4 particles/cm^3 at the downstream of DPF for the diesel engine during the cold start and transient operation. From the gasoline engine test, particle number concentration levels were analyzed at a a maximum of 2.0E+7 particles/cm^3 during the cold start and fast transient operation.

4. Vehicle experimental results

4.1 Particle emission characteristics during transient and steady driving conditions

Fig. 10 shows the time-resolved particle emission characteristics during dynamic operation for gasoline and diesel vehicles. Maximum particle number concentrations during cold start were 7.5E+6 particles/cm^3 for the gasoline vehicle and 4.5E+5 particles/cm^3 for the diesel one. Particle emissions are related to engine speed, load, coolant temperature, aftertreatment temperature and many others. Particle number levels from the gasoline vehicle are higher than those from thediesel vehicle due to rapid engine speed acceleration during cold start in order to promote the catalyst light-off. Particle concentration levels were reduced to below 1.0E+3 particles/cm^3 for the gasoline engine after cold start. In contrast, particle emissions from the diesel vehicle equipped with DPF were constantly maintained at 1.0 ~ 2.0E+5 particles/cm^3 after cold start.

There are several particle deposition mechanisms in a filter. Specifically, nucleation mode particles are trapped in the filter by diffusion. Diffusion deposition occurs due to a particle emission concentration gradient (ΔC). Here, the Peclet (Pe) number is used to explain this characterization. Pe number can be an effective parameter in comparing filtration at low

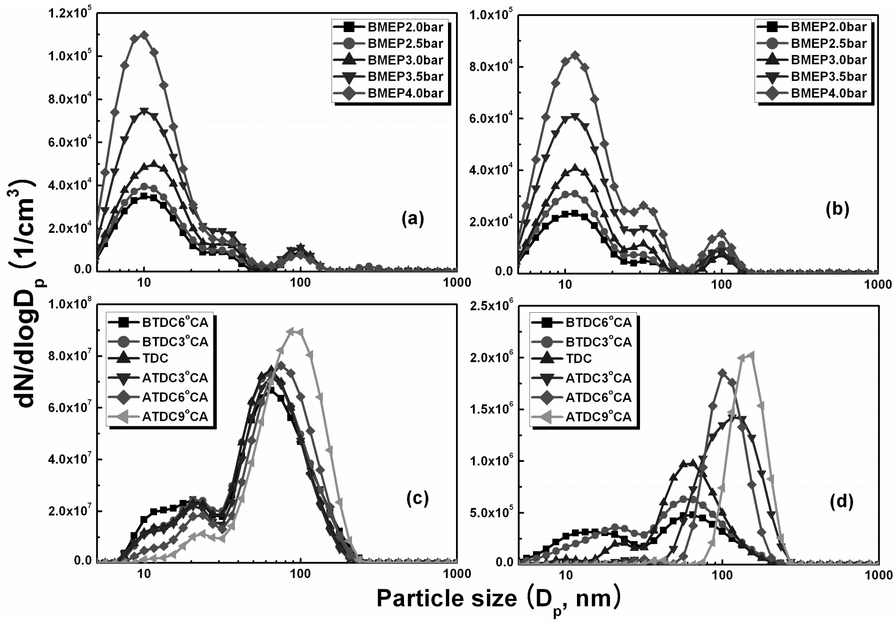

Fig. 7. Particle size distribution and number characteristics: (a) upstream of TWC; (b) downstream of TWC; (c) upstream of DPF; and (d) downstream of DPF. Test conditions are λ=1.0, S/A=MBT, 2,400 rpm and a fully warmed up condition for the gasoline engine and 1,400 rpm, BMEP 4.0 bar, and a fully warmed up condition for the diesel engine.

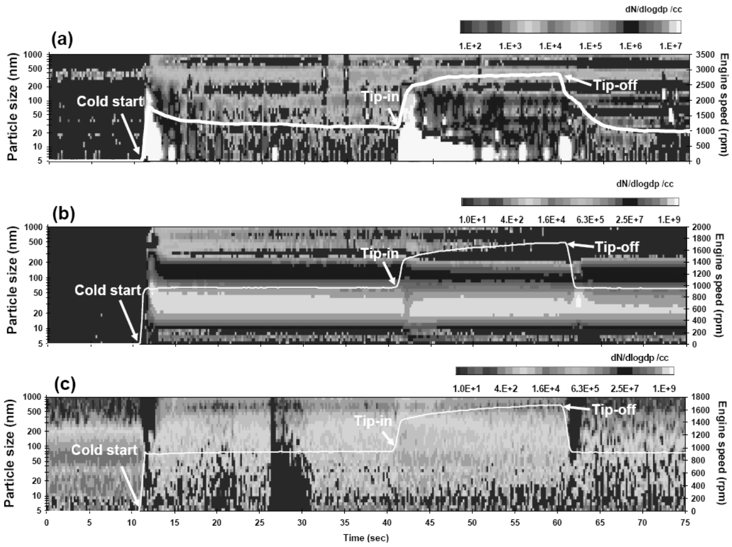

Fig. 8. Particle size spectra during the cold start and transient operation: (a) gasoline engine; (b) upstream of DPF for diesel engine; and (c) downstream of DPF for the diesel engine.

temperature DPF [20]. The filtration efficiency ($E_D = 2Pe^{-2/3}$) due to diffusion is a function of the dimensionless Pe number ($Pe = d_f U_0/D$). In addition, this parameter is inversely proportional to the diffusion coefficient (D) which increases with temperature [21]. Therefore, nucleation mode particles are not deposited on the filter surface emitted through the porous environment inside the filter. This is because the diffusion velocity ($V_D \sim D \cdot \Delta C$) of the particle is dropped due to insufficient DPF temperature.

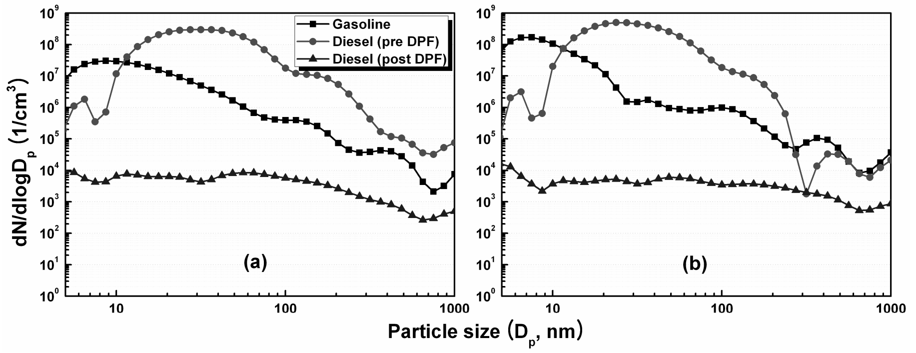

Fig. 9. Particle size distribution and number characteristics: (a) cold start and (b) transient.

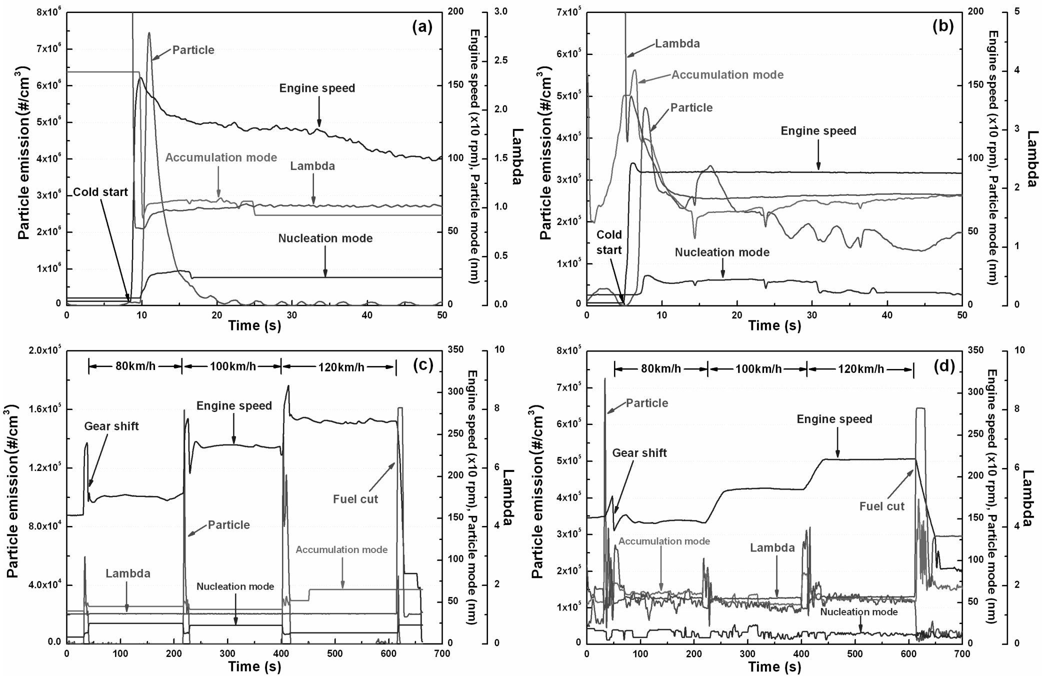

Fig. 10. Particle emission characteristics during dynamic operations with two vehicles: (a) cold start for the gasoline vehicle; (b) cold start for the diesel vehicle; (c) steady state for the gasoline vehicle; and (d) steady state for the diesel vehicle.

In the steady and transient test, particle concentrations sensitively increased with the variation of engine speed for gasoline and diesel vehicles. Especially, particle concentration levels were constantly maintained at 1.5E+5 ~ 2.0E+5 particles/cm^3 at a high speed condition (120 km/h). Particle emission from the diesel DPF vehicle at 120 km/h could be explained by the natural regeneration of particles (partial oxidation of loaded soot) brought about by the high temperature (measured temperature: 330ºC) inside the particulate trap during the high-speed operating condition.

4.2 Comparison of the continuous particle number concentration in the NEDC, FTP-75, and HWFET modes

Total particle number (N) emissions for the vehicle driving modes were calculated by means of the following equation in accordance with the particle number measurement procedure of Regulation No. 83 [22].

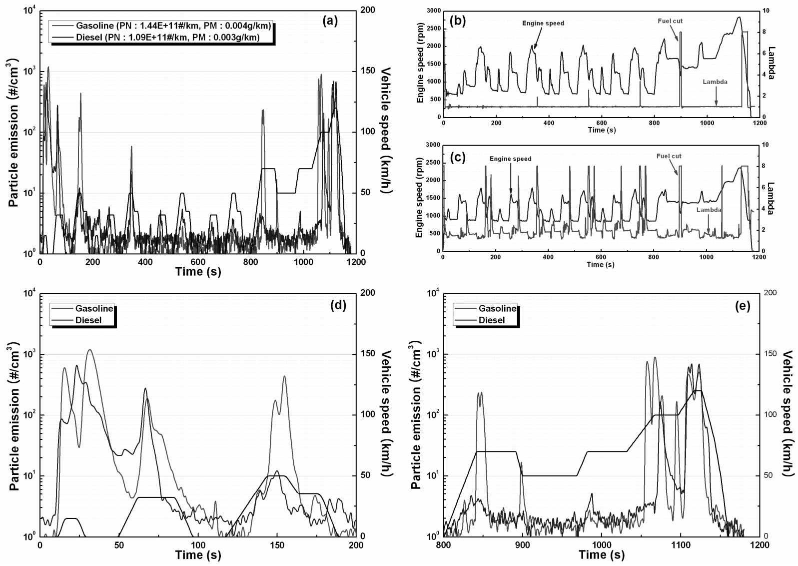

Fig. 11. Time-resolved particle number concentration characteristics during the NEDC mode with two vehicles: (a) NEDC mode; (b) Engine speed and lambda for the gasoline vehicle; (c) Engine speed and lambda for the diesel vehicle; (d) Cold ECE mode; and (e) EUDC mode.

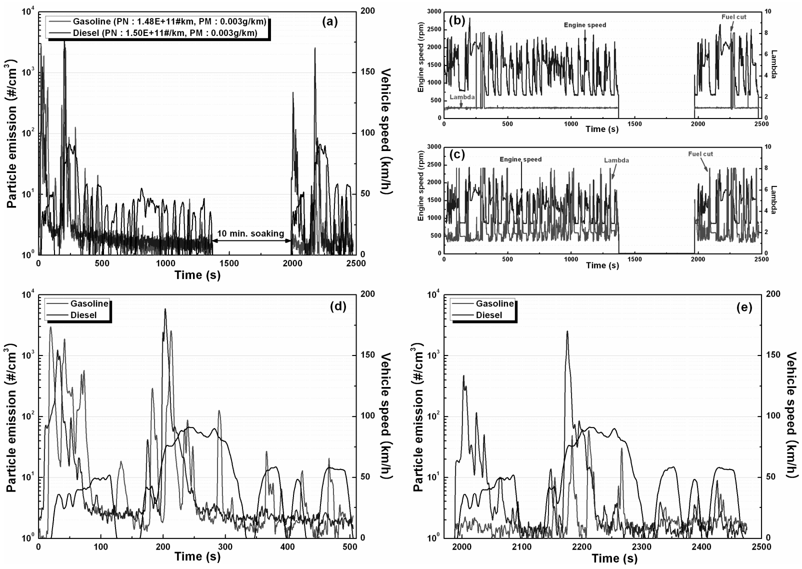

Fig. 12. Time-resolved particle number concentration characteristics during FTP-75 mode with two vehicles: (a) FTP-75 mode; (b) Engine speed and lambda for the gasoline vehicle; (c) Engine speed and lambda for the diesel vehicle; (d) Cold state (phase 1); and (e) Hot state (phase 3).

$$N = \frac{V_{mix} \times C_{avg} \times DR_{tot} \times 10^3}{d} \quad (1)$$

In Eq. (1), N (particles/km) is the particle number emission expressed in particle per kilometer, V_{mix} is the volume of the diluted exhaust gas in liter per test, C_{avg} is the average concentration of particles in diluted exhaust gas in particles per cubic centimeter, DR_{tot} is the total dilution factor of the diluter, and d is the distance corresponding to the test mode in kilome-

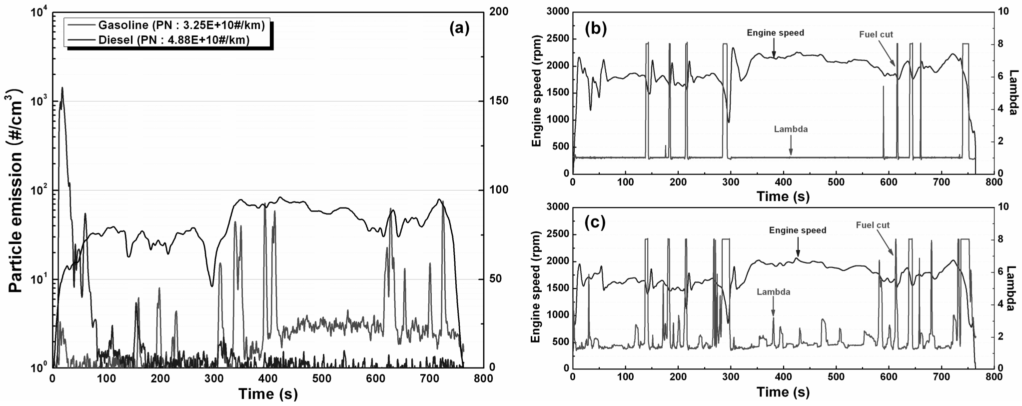

Fig. 13. Time-resolved particle number concentration characteristics during HWFET mode with two vehicles: (a) HWFET mode; (b) Engine speed and lambda for the gasoline vehicle; (c) Engine speed and lambda for the diesel vehicle.

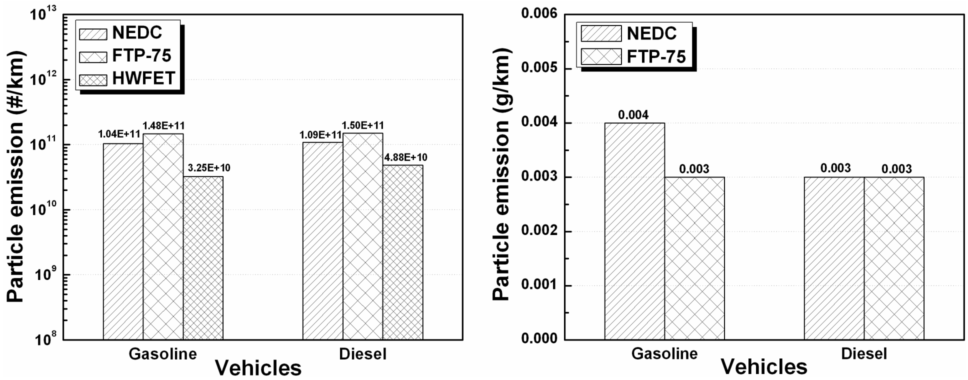

Fig. 14. Comparison of total particle number concentration and particle mass in different driving modes.

ter.

Fig. 11 shows the time-resolved particle emission traces measured by CPC for gasoline and diesel passenger vehicles in the NEDC mode. The levels of PM number emissions showed a close relationship with the driving condition of the vehicle testing modes. Particle number concentrations from gasoline and DPF diesel vehicles were highest during the cold start phase, whose level was 1.0E+3 particles/cm^3. After the engines warmed up, particle number concentrations were emitted by 2 ~ 4 particles/cm^3 at the all-accelerating duration for gasoline and diesel vehicles. Particle number concentrations emitted from gasoline and diesel increased along with the acceleration condition in the high-speed driving cycle, which was represented by the extra urban cycle.

Particle emissions were gradually reduced after the second mode of economic commission for Europe (ECE) 15 urban driving cycle and then maintained below 4 particles/cm^3, except for the accelerating duration of the extra urban driving cycle (EUDC) condition. Total particle number concentration and particle mass were 1.44E+10 particles/km and 0.004 g/km for the gasoline vehicle, respectively. On the other hand, those for the diesel vehicle were 1.09E+11 particles/km and 0.003 g/km, respectively. In the case of the diesel-fueled vehicle, the DPF system demonstrated a potential to reduce the particle number and mass emission enormously.

Fig. 12 presents the time-resolved particle emission behaviors of the FTP-75 mode. Particle formation increased in a manner similar to the NEDC mode during vehicle speed up. However, in this study, the concentrations were largely emitted at the cold state phase because the vehicle speed gradient was steeper than that for the NEDC mode. However, total particle number and mass of the FTP-75 mode showed similar levels compared to those of NEDC. To verify the vehicle speed effect on particle formation, the HWFET mode was also tested.

Fig. 13 represents the time-resolved particle emission behaviors of HWFET. Comparing NEDC and FTP-75 to the HWFET mode, the engine reached a fully warmed up condition and its average speed reached about 77.7 km/h (NEDC: 33.6 km/h, FTP-75: 34.1 km/h). The orders of particle number concentrations were 3.25E+10 ~ 1.50E+11 particles/km for the gasoline and diesel vehicles, respectively. The test results for total particle number concentration and particle mass are summarized in Fig. 14.

5. Closing remarks

This research aimed to evaluate the particle number and size distribution characteristics of the gasoline and diesel light duty vehicles which are meted by ULEV and EURO 4 regulations under different engine operating conditions and vehicle certification modes, such as NEDC, FTP-75, and HWFET. The PM size distribution measured in the gasoline and diesel engines was bi-modal, consisting of the nucleation and accumulation modes. The nucleation mode (d_p < 50 nm) in a gasoline engine was mainly emitted, while the accumulation mode (d_p > 50 nm) in a diesel engine was generated. As the spark timing for the gasoline engine became retarded, particle number concentration gradually decreased because of the oxidation of unburned fuel during the expansion stroke. However, as the fuel injection timing became retarded for the diesel engine, particle emissions were increased because of an incomplete combustion. The aftertreatment of the gasoline engine had a small effect on PM reduction at various part load conditions, and particle number concentration levels were reduced by a maximum of 3 orders of magnitude into the DPF downstream for the diesel engine.

Gasoline and diesel fueled vehicles, regardless of aftertreatment, both emit PMs during transient operation including cold start operation, heavy acceleration phase, and high speed period. In particular, particles were constantly emitted due to the natural regeneration of DPF in high-speed driving conditions. In addition, particle formation was dependent on the degree of transient operating cycle in the vehicle test modes, such as acceleration, deceleration, and vehicle speed. The order of magnitude of total particle concentrations with various test modes for gasoline and diesel shows similar levels. Particle concentration of the DPF diesel is below 6.0E+11 particles/km, which is well within the particle number emission regulations enacted at EURO 5 and EURO 6.

Acknowledgments

This research was supported by the Korea Petroleum Association and the ECO-STAR Project of the Korea Ministry of Environment.

References

[1] D. Dockery, C. Pope and X. Wu, An association between air pollution and mortality in six US cities, *New England Journal of Medicine*, 329 (24) (1993) 1753-1759.

[2] B. Ostro, A research for a threshold in the relationship of air pollution to mortality: a reanalysis of London winters, *Environmental Health Perspectives*, 58 (1984) 397-399.

[3] C. Pope, J. Schwartz and M. Ransom, Daily mortality and PM_{10} pollution in Utah Valley, *Archives of Environmental Health*, 47 (3) (1992) 211-217.

[4] K. Vaaraslahti, J. Keskinen, B. Giechaskiel, T. Murtonen and A. Solla, Effect of lubricant on the formation of heavy-duty diesel exhaust nanoparticles, *Environmntal Science and Technology*, 39 (2005) 8497-8504.

[5] B. Giechaskiel, R. Munoz-Bueno, L. Rubino, U. Manfredi, P. Dilara and G. D. Santi, Particulate Measurement Programme (PMP): Particle size and number emissions before, during and after regeneration events of a Euro 4 DPF equipped light-duty diesel vehicle, *SAE Paper* No. 2007-01-1944 (2007).

[6] J. R. Hagena, Z. S. Filipi and D. N. Assanis, Transient diesel emission, analysis of engine operation during a tip-In, *SAE Paper* No. 2006-01-1151 (2006).

[7] M. Y. Kim and C. S. Lee, Effect of a narrow fuel spray angle and a dual injection configuration on the improvement of exhaust emissions in a HCCI diesel engine, *Fuel*, 86 (2007) 2871-2880.

[8] C. W. Wu, R. H. Chen, J. Y. Pu and T. H. Lin, The influence of excess air ratio on engine performance and pollutant emission of an SI engine using ethanol-gasoline-blended fuels, *Atmospheric Environment*, 38 (2004) 7093-7100.

[9] D. B. Kittelson, Engines and nanoparticles: A review, *Journal of Aerosol Science*, 29 (5/6) (1998)

575-588.
[10] B. Campbell, M. Peckham, J. Symonds, J. Parkinson and A. Finch, Transient gaseous and particulate emissions measurements on a diesel passenger car including a DPF regeneration event, *SAE Paper* No. 2006-01-1079 (2006).
[11] D. Kayes and S. Hochgreb, Mechanism of Particulate Matter Formation in Spark-Ignition Engines, *Environmental Science and Technology*, 33 (1999) 3957-3967.
[12] J. Andersson, B. Wedekind, D. Hall, R. Stradling and C. Barnes, DERT/SMMT/CONCAWE Particle Research Programme: Light-duty results, *SAE Paper* No, 2001-01-3577 (2001).
[13] J. Andersson, D. Clarke and J. A. Watson, UK Particulate Measurement Programme (PMP): A near US 2007 approach to heavy duty diesel particulate measurements - comparison with the standard European method, *SAE Paper* No. 2004-01-1990 (2004).
[14] J. Andersson, B. Giechaskiel, R. Munoz-Bueno, E. Sandbach and P. Dilara, *Particle Measurement Programme (PMP) light-duty inter-laboratory correlation exercise (ILCE-LD) final report*, JRC, EU (2007).
[15] C. L. Myung, H. Lee, S. Kwon, S. Lee, J. Jun, Y. Lee, Y. Woo, M. Lee, G. N. Bae and S. Park, Interlaboratory correlation exercise on a light-duty diesel passenger vehicle to verify nano-particle emission characteristics by Korea particle measurement program, *Journal of Mechanical Science and Technology,* 23 (2009) 729-738.
[16] J. W. Lee, Y. I. Jung, M. W. Jung, K. O. Cha, S. I. Kwon, J. C. Kim and S. Park, Experimental investigation and comparison of nano-particle emission characteristics in light-duty vehicles for two different fuels, *International Journal of Automotive Technology*, 9 (4) (2008) 397-403.
[17] C. Roberto, S. Volker, V. Rainer and B. Thorsten, Measurement of nucleation and soot mode particle emission from a diesel passenger car in real world and laboratory in situ dilution, *Atmospheric Environment*, 41 (2007) 2125-2135.
[18] Bosch, *Diesel engine management*: *An overview*, Robert Bosch GmbH, Germany, (2003) 52-53.
[19] G. B. Parvate-Patil, H. Hong and B. Gordon, An assessment of intake and exhaust philosophies for variable valve timing, SAE paper No. 2003-32-0078 (2003).
[20] E. Wirojsakunchai, E. Schroeder, C. Kolodziej, D. E. Foster, N. Schmidt, T. Root, T. Kawai, T. Suga, T. Nevius and T. Kusaka, Detailed diesel exhaust particulate characterization and real-time DPF filtration efficiency measurements during PM filling process, *SAE Paper* No. 2007-01-0320 (2007).
[21] W. C. Hinds, *Aerosol technology 2nd Edition*, John Wiley & Sons, New York, (1999) 191-196.
[22] TRANS-WP29-GRPE-48. Conclusions on Improving Particulate Mass Measurement Procedures and New Particle Number Measurement Procedures Relative to The Requirements of The 05 Series of Amendments to Regulation No. 83, http://www.unece.org/trans/doc/2004/wp29grpe.

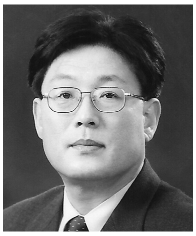

Simsoo Park received his B.S. and M.S. degrees from Seoul National University in 1977 and 1979, respectively, and a Ph.D. from the State University of New York at Stony Brook. He served as a Chief Research Engineer at Hyundai Motor Company, a Director for Publication of the KSME, a Technical Advisor of Hyundai-Kia Motor Company, and an Editing Director, Project Director, International Director, Accounting Director, and General Affair Director of KSAE. He is currently Vice President and Editor-in-Chief of IJAT at KSAE and a professor in school of mechanical engineering at Korea University.

Hyungmin Lee received his B.S. degrees from Republic of Korea Naval Academy in 1997 and his M.S. degrees from Korea University in 2005, respectively. He served as an Operation Officer, Command Engineer Officer at various naval vessels. He is currently Ph.D. course in school of mechanical engineering at Korea University and his rank is a Lieutenant Commander of Korea Navy.